

Cellular Neural Networks - An Analogous Model for Stress Analysis of Prismatic Bars Subjected to Torsion

Ivan Krstić

Assistant Director

Federal Institution for Standardization
Belgrade

Dragan Kandić

Professor

University of Belgrade
Faculty of Mechanical Engineering

Branimir Reljin

Professor

University of Belgrade
Faculty of Electrical Engineering

In the most general case finding the shear stress distribution on the cross-section of prismatic bar subjected to torsion presents a serious problem that can be solved in two steps. The first of them consists in finding the stress function, while the second one consists in finding the shear stress distribution by using this function. The stress function appears to be the solution of Poisson's partial differential equation for the given conditions of unambiguity, which in the theory of elasticity describes torsion of prismatic bars in terms of stresses. The modeling by means of electric networks is one of the few possible means for finding the stress functions. This paper describes the method the cellular neural networks can successfully be applied as analogous models in finding stress functions of twisted prismatic bars with complex polygonal cross-sections. The stress functions produced in this way are straightforwardly applicable in calculation of resulting shear stress distributions. The effectiveness of the proposed method is demonstrated through the selected illustrative examples. The method is applicable in various branches of mechanical engineering, as well.

Keywords: modeling, stress analysis, torsion, prismatic bar, cellular neural network

1. INTRODUCTION

Various parts of machines, vehicles and general metal constructions can have forms of prismatic bars (bars with solid polygonal cross-sections), or sometimes the prismatic bars can be assumed as approximations of such parts. The prismatic bars can often be subjected to torsion (twisting). The torsion describes the action causing the bar to twist, as is depicted in Fig. 1. This can be caused by applying a torque (a couple of forces) acting about longitudinal axis of a bar – when the pure torsion occurs, or by the application of transverse loads – when the torsion simultaneously occurs with bending. The angle through which the observed end of the bar twists is called the twist angle and is usually small. In addition, the torsion can be elastic and plastic. The consideration developed in this paper relates only to the elastic torsion of prismatic bars subjected to the pure torsion.

The usual designer's tasks include calculations of allowed loads, of maximum stresses (or deformations) and/or of dimensions. For each of them it is necessary to know the relations connecting load, stress, dimensions, deformation and material properties. Principles used to set up these relations are subject of investigation of the theory of elasticity - a branch of mathematical physics. The practical part of the theory of elasticity is strength of materials.

Usually, the main goal in calculations of prismatic bars is to find the maximum shear stresses or, generally

speaking, the stress distribution for given loads. Only a small number of relatively simple problems can be solved analytically, by using formulas from the strength of materials. They relate either to cylindrical bars (i. e. bars with circular cross-sections), or to prismatic bars having the cross-sections in the shape of basic geometrical figures. Consequently, there arises the need for development of a new class of indirect methods for stress analysis of twisted prismatic bars.



Figure 1. Twisted prismatic bars of different cross-sections.

The complexity of the stress analysis related to torsion of prismatic bars will be more obvious, if we firstly recall the simplest case - the elastic torsion of a solid cylindrical bar made from isotropic material. When the cylindrical bar twists it is assumed that all cross-sections remain plane and normal to the longitudinal axis of the bar (in other words, there is no warping), radial lines remain straight, and the deformation occurs only by one cross-section twisting relative to another. Thereby, in cross-sections occur only shear stresses. It is assumed that distribution of shear stress is uniform in all cross-sections, including, also, the extreme sections of the bar. In conclusion, the stress analysis of twisted cylindrical bars is quite simple since the shear stress varies linearly with radius from zero - at the center of the twist (i. e. the center of the cross-section) to maximum value-at points which are mostly remote from the center of twist, that lie at the outer radius R (Fig. 2).

The center of the twist is a point about which the whole cross-section twists when subjected to torsion. This is also called the shear center, since it is the point

Received: September 2002, accepted: March 2003.

Correspondence to: Ivan Krstić,
Federal Institution for Standardization, Kneza Miloša 200,
11000 Belgrade, Serbia and Montenegro,

E-mail: ivkrstic@EUnet.yu

of the cross-section where the transverse (shear) loads produce pure bending of bar, without torsion.

If the cross-section has an axis of symmetry (as, for example, semicircle, segment of a circle, sector, isosceles triangle, etc.), then the center of twist lies along that axis (whose location is calculated by means of the well known formulas), but it does not coincide with the centroid of the cross-section. If the cross-section has more than one axis of symmetry (as, for example, circle, ellipse, equilateral triangle, rectangle), then the center of twist lies at intersection of the axes of symmetry and it coincides with centroid of the cross-section. However, the location of the center of twist in an irregular non-circular solid cross-section is unknown in advance, and cannot be calculated on some elementary way.

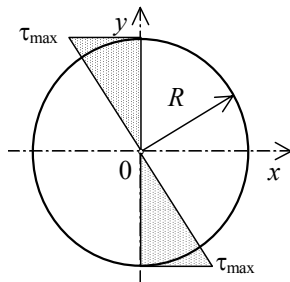


Figure 2. The distribution of the shear stress on the cross-section of a cylindrical bar.

The observations made for the elastic torsion of cylindrical bars do not hold for those of prismatic bars. The theory of elasticity has been applied to finding the analytical solutions of torsion for the case of prismatic bars. Saint-Venant was the first one who accurately has described the shear stress distribution on the cross-section of a non-circular bar by using the theory of elasticity (*Barré de Saint-Venant, Mémoire sur la torsion des prismes, 1855*).

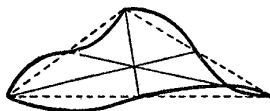


Figure 3. The warping of an equilateral triangular cross-section (according to [1]).

The distribution of shear stress in twisted prismatic bars is more complex than distribution in twisted cylindrical bars. There is a few reasons for this. The shear stress is not constant at a given distance from the center of twist since it depends on coordinates x and y (not on radius). The consequence of this is the warping of cross-sections, as depicted in Fig. 3. Then the maximum shear stresses does not appear at the points most remote from the center of twist. In addition, the theory of elasticity shows that the shear stress at the corners of twisted polygonal cross-sections is zero. Consequently, the stress analysis of twisted prismatic bars is, also, more complex than those of cylindrical bars [1]–[3].

The maximum shear stress on the solid cross-section in the shape of a non-circular geometrical figure, τ_{max} , is calculated from the following expression:

$$\tau_{max} = T / W_k, \quad (1)$$

where T is torque (external torsional load) and W_k the so-called modified section modulus of cross-sectional area.

The total angle of twist (in radians), φ_T , for a given torsional torque and length of the bar can be calculated by using the following expression:

$$\varphi_T = \frac{TL}{GI_k}, \quad (2)$$

where L is the length of bar, G is the modulus of rigidity (shear modulus) of material, and I_k is the so-called torsional moment of the cross-sectional area. As an example, for steels G amounts approximately $7.8 \cdot 10^5 \text{ daN/cm}^2 - 8 \cdot 10^5 \text{ daN/cm}^2$.

For the cross-sections in shape of basic non-circular geometrical figures, the values of W_k and I_k can be calculated by means of the well known formulas. It should be kept in mind that the value of I_k equals to the value of the second polar moment of the cross-sectional area and the value of W_k equals the value of the section modulus of cross-sectional area, only for circular cross-sections.

Let us now take, for instance, a prismatic bar with rectangular cross-section having sides b and h , whereby $h/b \geq 1$. When such a bar is subjected to torsion, the theory of elasticity shows that the maximum shear stress occurs at the middle of each long side (Fig. 4). In addition, the shear stresses at the corners and center of the cross-section equal zero, and the stress variations on the cross-section are primarily nonlinear. The shear stress in the middle of each short side can be calculated by using the formula $\tau_1 = k_1 \tau_{max}$. The value of τ_{max} is calculated by means of (1), whereby W_k is given by $W_k = k_2 Fb$, with $F = bh$. In a similar way, the value of φ_T is calculated by means of (2), whereby I_k is given by $I_k = k_3 Fb^2$. In the last three stated formulas k_1 , k_2 and k_3 are the Saint-Venant coefficients whose values are known for different values of ratio h/b . For instance, in the case of the square cross-section ($h/b=1$) it holds: $k_1=1$, $k_2=0.208$ and $k_3=0.1406$.

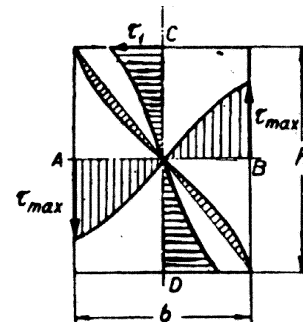


Figure 4. Classical presentation of distribution of shear stresses on the cross-section of a twisted prismatic bar with rectangular cross section (according to [3]).

However, for an arbitrary solid cross-section, say in the shape of an irregular polygonal geometrical figure, neither the values of I_k and W_k , nor the values of maximum shear stress and angle of twist can be calculated on an elementary way. Therefore, in such cases, the shear stress distribution is to be found directly, by using experiments, or indirectly, by solving the general partial differential equation describing the torsion of prismatic bars in the theory of elasticity.

The methods of experimental stress analysis include electrical resistive strain gauges, photo elasticity, brittle coatings, laser speckle interferometry, etc. [4]. Today, mainly the strain gauges are used. However, each of the mentioned methods requires the surface treatments and/or modifications that can change mechanical properties on the local level, or requires the complex, intensive and expensive preparation and equipment. Furthermore, the experiments can take a lot of time and valuable development time can be lost if they have to be repeated after each improvement of design. That is why the detection of weak points in the design can significantly reduce the development and testing time. Since detection of weak points in an early stage of design is quite limited with traditional measuring techniques, any method to find the shear stress distribution by solving formerly mentioned partial differential equation of the torsion is preferred from the designer's point of view.

The previously mentioned general equation can be solved either numerically, or by means of the analogous models. Today, it is usually solved numerically, by means of fast general-purpose digital computers. In spite of the many well known advantages, the numeric methods sometimes require a lot of time, since they are based on iterative solving procedures. However, solving the same equation by means of analogous models is very efficient and accurate method frequently used in research practice. In this case, the modeling can be carried out by means of the structure-continual models (mechanical or hydro-mechanical models) or by means of the structure-discrete models (electrical networks).

Almost a hundred years ago, Prandtl has published his famous membrane (or the so-called hydro-mechanic) analogy of the torsion problem (*Ludwig Prandtl, Zeitschrift für Physik, Vol. 4, 1903*), where he showed that by using a flexible membrane (or the so-called soap film method) the stress distribution in torsion could be obtained experimentally. However, because of simple physical realization and data acquisition, the modeling by means of electric networks is more convenient than modeling by means of mechanical models. In the past, various space and space-time problems were modeled and solved by means of electric R- or RC-networks [5], [6]. Nowadays, the cellular neural networks (CNNs) [7], [8], as their variants also, are mostly used for the same purpose. The CNNs are proved to be very convenient and successful means in solving problems related to the mechanical vibrating systems [9]–[11], heat transfer [12]–[14], fluid flow [15], and other similar subjects.

This paper aims to present the way the CNNs can be successfully applied as analogous models in the first step of finding the shear stress distribution in the twisted prismatic bars. The mathematical definition of problem is given in the second section of the paper. This is then followed by discretization of problem in the third section. The architecture of CNN which serves as analogous model and original-model analogy are briefly described in the fourth section, while the results of modeling of the three selected problems and relevant comments are given in the fifth section of paper. Finally, the conclusions are drawn out in the sixth section of paper.

2. DEFINITION OF PROBLEM

From the theory of elasticity, it is well known that the torsion of prismatic bars is described in terms of stresses, by Poisson's partial differential equation of the second order:

$$\frac{\partial^2 \Phi}{\partial x^2} + \frac{\partial^2 \Phi}{\partial y^2} = -2G\varphi, \quad (3)$$

where Φ is continual function called the *stress function*, and φ is the angle of twist per unit length ($\varphi = \varphi_T/L$). It can be shown that when the solid cross-section of bar (without inner cavities) is bounded by a closed contour, the finding of stress-function is reduced to the classical problem of integrating (3) with the boundary condition:

$$\Phi|_b = 0. \quad (4)$$

The solution of (3) is stress function $\Phi(x,y)$ which identically satisfies the same equation and (4). The physical essence of this function is easily explainable by using Prandtl's membrane analogy.

From the theory of elasticity, it is also well known that the surface of a deflected flexible, inextensible membrane is described by Poisson's equation:

$$\frac{\partial^2 z}{\partial x^2} + \frac{\partial^2 z}{\partial y^2} = \frac{p}{Q}, \quad (5)$$

where z is the ordinate of the surface of membrane, p is the uniform pressure (continually distributed external load) to the membrane, and Q is the magnitude of the constant tension of membrane per unit length of section of the membrane. There is no need to explain that the boundary condition should read:

$$z|_b = 0. \quad (6)$$

By comparing (3) with (5), as also (4) with (6), it is easy to observe their isomorphism. Therefore, if values of p and Q in (5) are selected so that the value of ratio p/Q is proportional to the value of product $2G\varphi$ in (3), then it is obvious that the value of z is proportional to Φ . In other words, the surface described by function Φ will have the shape of deflected membrane which is clamped over the frame with the same contour as cross-section of the bar and is exposed to the same load.

The shape of the deflected membrane helps in visualization of stress distribution in the twisted bar. Lines of equal deflection on the membrane correspond to shear stress lines of the twisted bar. The direction of a particular shear stress resultant at a point is at right angle to the maximum slope of the membrane at the same point. The slope of the deflected membrane at any point with respect to the plane xOy is proportional in magnitude to the shear stress at the corresponding point on the cross-section of the bar. Since the slope is zero at the very top of the membrane, the shear stress is zero at the same location on the cross section of the bar (i. e. the center of the twist).

Consequently, the function Φ has two important features. The first one is that its partial derivatives with respect to coordinates y and x represent components of the shear stress τ :

$$\tau_x = \frac{\partial \Phi}{\partial y}, \quad \tau_y = \frac{\partial \Phi}{\partial x}, \quad (7)$$

where τ_x is the shear stress component in direction of x -axis and τ_y is the shear stress component in direction of y -axis. The second feature is that the torque T is equal to the twice of volume bounded by surface described by function Φ and the cross-section area in the xOy plane:

$$T = 2 \iint_{(F)} \Phi \, dF. \quad (8)$$

The proof of the last two statements will not be given here because of complexity and since it can be found in textbooks on the theory of elasticity (for instance, in [1], or elsewhere).

In conclusion, to find the shear stress distribution in the cross-section of the twisted prismatic bar, that is the function $\tau(x,y)$, firstly the stress function Φ has to be determined. This function can be found if (3) is modeled and solved, for instance, by means of a CNN. When the numeric values of the stress function are obtained then the stress components τ_x and τ_y should be calculated numerically by using (7) and finally the resultant shear stress τ can be determined through the simple arithmetic operations.

3. DISCRETIZATION OF PROBLEM

The necessary condition to model and solve the proposed problem by means of a CNN (or by a traditional electric network) is spatial discretization and suitable approximation of (3). Usual way to achieve this goal is the well-known finite difference method. Very effective and efficient discretization and approximation is achieved by finite differences scheme depicted in Fig. 5. If the partial derivatives on left side of (3) are replaced by approximations of the second order derived by using the mentioned scheme, the following set of linear algebraic equations is obtained:

$$\frac{\Phi_{i+1,j} - \Phi_{i,j}}{a^2} + \frac{\Phi_{i-1,j} - \Phi_{i,j}}{a^2} + \frac{\Phi_{i,j+1} - \Phi_{i,j}}{a^2} + \frac{\Phi_{i,j-1} - \Phi_{i,j}}{a^2} = -2G\varphi, \quad (i,j) \in W. \quad (9)$$

In (9) Φ_{ij} is the approximation of continuous function $\Phi(x, y)$ in node (i,j) , a is the step of the square grid (that is, the distance between the central node (i,j) and the neighbour node (k,l) in corresponding direction Ox or Oy), while W denotes a finite set of grid nodes bounded by the contour of the bar cross-section.

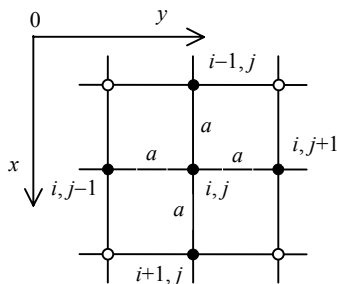


Figure 5. The finite differences scheme "4+1".

After a simple rearrangement, (9) can be rewritten in the well-known discrete "cellular" form:

$$-\frac{4}{a^2} \Phi_{i,j} + \sum_{(k,l) \in N_r(i,j)} \frac{1}{a^2} \Phi_{k,l} + 2G\varphi = 0, \quad (i,j) \in W. \quad (10)$$

Relation (10) holds for all grid nodes lying in the cross-section. However, for those grid nodes lying on boundary (contour) of the cross-section, relation (10) reduces to the following discretized boundary condition:

$$\Phi_{i,j}|_b = 0, \quad (i,j) \in W. \quad (11)$$

4. THE ARCHITECTURE OF THE CNN AND ORIGINAL-MODEL ANALOGY

The CNNs are powerful computing structures for diverse computing operations in discrete N -dimensional space. These operations are simultaneously performed by a huge number of locally connected artificial neurons called cells, placed in nodes of a regular geometric grid. CNNs belong to a great family of electronic structures, commonly called the *artificial neural networks*.

The CNNs have been developed in 1988 by L. O. Chua and L. Yang from University of California, Berkeley, and primarily were intended for image processing and pattern recognition purposes. The paradigm of CNN can be assumed as product of evolution of cellular automata. In addition, CNNs are universal and equivalent to the Turing's machine.

The cells in CNNs can be ordered in a single plane (that is, in the nodes of a two-dimensional, orthogonal, triangular, or hexagonal grid), or in space (that is, in the nodes of a three-dimensional, orthogonal, or cylindrical grid). The planar (i. e. two-dimensional) CNNs are called *single-layer CNNs*, and spatial (three-dimensional) CNNs are called *multi-layer CNNs*.

The cells are assumed as simple analog processors consisting of standard elements of electric and electronic circuits. The CNNs operate iteratively and thus they belong to the class of recurrent networks. Main feature of CNNs, as well as basic difference in relation to other paradigms of artificial neural networks, is the local connectivity of cells. Each cell in the CNN is regularly connected only with the cells from a defined set that is called neighborhood and is denoted by $N_r(i,j)$. The size of the neighborhood is defined by radius r , which can take different integer values starting from one. In special case, the radius can assume such a value so that neighborhood of each cell comprises all other cells in CNN. That CNN becomes Hopfield's neural network, wherein each neuron is connected with all others. With respect to the physical (i. e. electronic) implementation of a CNN, the most desirable dimension of radius appears to be one.

Due to local connectivity of cells and well-defined, continual dynamics, the CNNs are very suitable both for modeling of space and space-time physical processes and for electronic implementation of models by means of discrete circuit elements, or VLSI technology. Continuous functions describing such processes are space discretized in CNN by using finite number of locally connected cells, while time-continuous dynamics of CNN is used to simulate the dynamical behavior of continuous functions. Due to the collective and simultaneous activity of all cells, simulation by using analogous CNNs is

incomparable faster than the sequential simulation implemented on the general-purpose digital computers.

Without any loss of generality, the concept of CNNs can be explained by the orthogonal single-layer CNN with $M \times N$ cells that are placed in the nodes of square grid having M rows in direction of x -axis ($0x$) and N columns in direction of y -axis ($0y$) (Fig. 6). The cell in the i -th row and the j -th column is denoted by $C(i, j)$. With respect to their position in CNN, the cells $C(1, j)$ and $C(M, j)$ ($1 \leq j \leq N$) and cells $C(i, 1)$ and $C(i, N)$, ($1 \leq i \leq M$) are called *boundary cells* and all other cells $C(i, j)$, ($1 < i < M$; $1 < j < N$) are called *inner cells*.

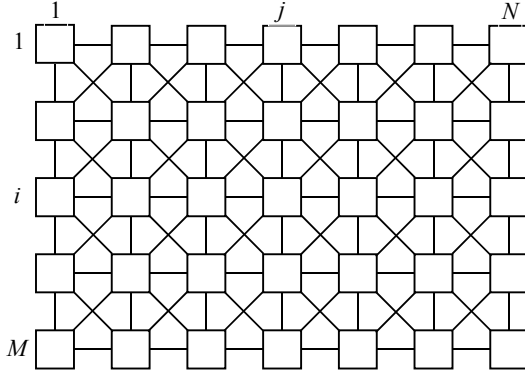


Figure 6. The single-layer orthogonal cellular neural network of dimension $M \times N$.

The typical electric circuit of the cell $C(i, j)$ in CNN is depicted in Fig. 7. The CNN state is described by the following set of equations of cell circuits:

a) State equation

$$C \frac{dv_{xij}(t)}{dt} = -\frac{1}{R_x} v_{xij}(t) + \sum_{(k,l) \in N_r(i,j)} A(i, j; k, l) v_{ykl}(t) + \sum_{(k,l) \in N_r(i,j)} B(i, j; k, l) v_{ukl} + I, \quad i=1, \dots, M, \quad j=1, \dots, N; \quad (12a)$$

b) Equation of output

$$v_{yij}(t) = \frac{1}{2} \left[|v_{xij}(t) - V_o| - |v_{xij}(t) + V_o| \right], \quad V_o \geq 1, \quad i=1, \dots, M, \quad j=1, \dots, N; \quad (12b)$$

c) Equation of input

$$v_{uij} = E_{ij}, \quad E_{ij} \geq 0, \quad i=1, \dots, M, \quad j=1, \dots, N. \quad (12c)$$

In (12a)–(12c) C is the capacitance of linear capacitor, R_x is the resistance of linear resistor, $A(i, j; k, l)$ is the feedback operator, $B(i, j; k, l)$ is controlling operator, E_{ij} is voltage of independent voltage source, and I is current of independent current source. The voltages v_{xij} , v_{yij} and v_{uij} are called the state, output and input, respectively. The output characteristic of cell $v_y = f(v_x)$ is a piecewise linear function having the unity slope in the interval $[-V_o, V_o]$, as is depicted in Fig. 8.

In our case, we can use the same orthogonal single-layer CNN depicted in Fig. 6 to solve discretized problem described by (10) and (11). However, to that purpose the cells in CNN can only be four-connected (that is without the diagonal connections).

In the stable equilibrium state of CNN, the left sides of (12a) must be zero. Then, under conditions $[B(i, j; k,$

$l)=0, E_{ij}=0, A(i, j; i, j)=0]$ for $\forall(i, j)$ and $\forall(k, l)$, it is easy to observe direct analogy between mathematical models (10) and (12a). Thus the following proportions can be set up: $S_\Phi = \Phi_{ij}/V_{xij} = \Phi_{kl}/V_{ykl}$, $S_R = a^2/(4R_x) = a^2 A(i, j; k, l)$ and $S_Q = 2G\Phi/I$, where V_{xij} and V_{ykl} are stable state values of voltages v_{xij} and v_{ykl} , respectively, while S_Φ , S_R and S_Q are model scales. The physical similarity between the original and the model is provided if the parameters of the CNN cell are selected in such a way so that the model scales satisfies the similarity criterion $S_\Phi/S_R = S_Q$.

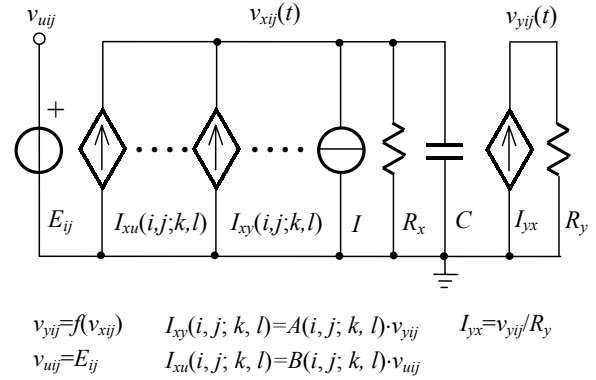


Figure 7. The typical cell circuit $C(i, j)$.

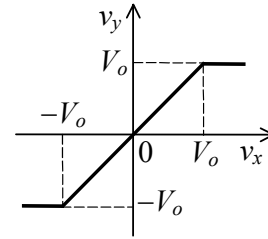


Figure 8. The output characteristic $v_{yij} = f(v_{xij})$.

If the CNN and the discretized cross-section of bar are geometrically and physically similar and if only the linear part of characteristic $v_{yij} = f(v_{xij})$ is used, then (10) – and thus with (3) – can be modeled and solved by using CNN defined with (12a)–(12c).

By taking into account the established similarities of the mechanical and electric quantities, as well as (7), the numerical value of shear stress $\tau_{i,j}$ in the grid node (i, j) will be given by the following expression:

$$\tau_{i,j} = \sqrt{\tau_{xi,j}^2 + \tau_{yi,j}^2} = \frac{S_\Phi}{a} \sqrt{\Delta V_{yij}^2|_y + \Delta V_{yij}^2|_x}, \quad (i, j) \in W, \quad (13)$$

where, $\Delta V_{yij}|_x = |V_{yi(i+1)} - V_{yij}|$ and $\Delta V_{yij}|_y = |V_{y(i+1)j} - V_{yij}|$. In addition, by taking into account (8), the torque T can be determined by using the relation:

$$T \approx 2a^2 \sum_{(i,j)} \Phi_{i,j} = 2S_\Phi a^2 \sum_{(i,j)} V_{yij}, \quad (i, j) \in W. \quad (14)$$

Relations (13) and (14) can be used to calculate the non-dimensional coefficient:

$$K_{i,j} = \frac{\tau_{i,j} b^3}{T} = n^3 \frac{\sqrt{\Delta V_{yij}^2|_y + \Delta V_{yij}^2|_x}}{2 \sum_{(k,l)} V_{ykl}}, \quad (i, j) \in W, \quad (15)$$

where b is characteristic dimension of the cross-section,

through which all other dimensions of the cross-section can be expressed in non-dimensional form, and n is the number of grid steps along dimension b ($b=n \cdot a$). This coefficient is very useful, since it enables calculation of shear stress values at any specific point (including τ_{\max}), for the given torque T and geometrical parameter b , without any further modeling.

5. RESULTS AND COMMENTS

The presented method of modeling was tested in solving a number of problems, but its power will be demonstrated here only on the following three illustrative examples.

Example 1. Find the shear stress distribution in the steel bar ($G=8 \cdot 10^5$ [daN/cm²]) of length $L=100$ [cm], with solid cross-section of the square shape with side $b=7$ [cm], which is twisted for the angle $\varphi_T=1^\circ 30'$.

The cross-section of the bar was discretized by a square grid with step size $a=5$ [mm] and in this way 225 grid nodes was obtained, in total. The discretized cross-section was modeled by a CNN with dimensions $M=15$ and $N=15$, that is by 225 cells, in total. Thus, the model (CNN) and the original (the discretized cross-section) are produced geometrically similar. The values of cell parameters are: $A(i, j; k, l)=200$ [μS], $R_x=1.25$ [k Ω], $I=10$ [mA] and $C=5$ [μF]. The steady-state cell outputs obtained through simulation process are recorded and later multiplied by the actual value of scale S_Φ . In this way the numerical values of stress function approximations $\Phi_{i,j}$ are obtained and are represented in Fig. 9a by a 3D plot. Therefrom it becomes obvious that the discretized form of continuous, smooth and symmetric function Φ corresponds to deflected square membrane. All previous facts justify the correctness of the proposed way of modeling and the applied simulation procedure.

The fact that the considered problem is solvable analytically, enables a direct comparison between the obtained results and exact analytical solution. The accuracy of the obtained values for $\Phi_{i,j}$ is assessed indirectly, by means of relative error of resulting torque calculated from (14). In that way it was found that the relative error of torque amounts only about 1.6 %, that is quite acceptable.

Consequently, the numerical values of shear stress approximations $\tau_{i,j}$ were obtained and are represented in Fig. 9b, also by a 3D plot. In Fig. 9b it is depicted that the maximum shear stresses of the same magnitude occur at nodes (1,8), (8,1), (8,15) and (15,8), which coincide with middle points of the respective cross-section sides. In addition, the shear stress at corner nodes (1,1), (1,15), (15,1), (15,15) and the central node (8,8) appears to be zero. This result is physically correct and is in accordance with the presentation in Fig. 4 and results obtained by known formulas from strength of materials.

However, the relative error of the shear stress is slightly greater than the relative error of the stress function and it amounts to around 5 %. Of course, it can be reduced to the acceptable level by generating model of greater order than this applied. It should be kept in mind that the aim of this test was not to impress the people

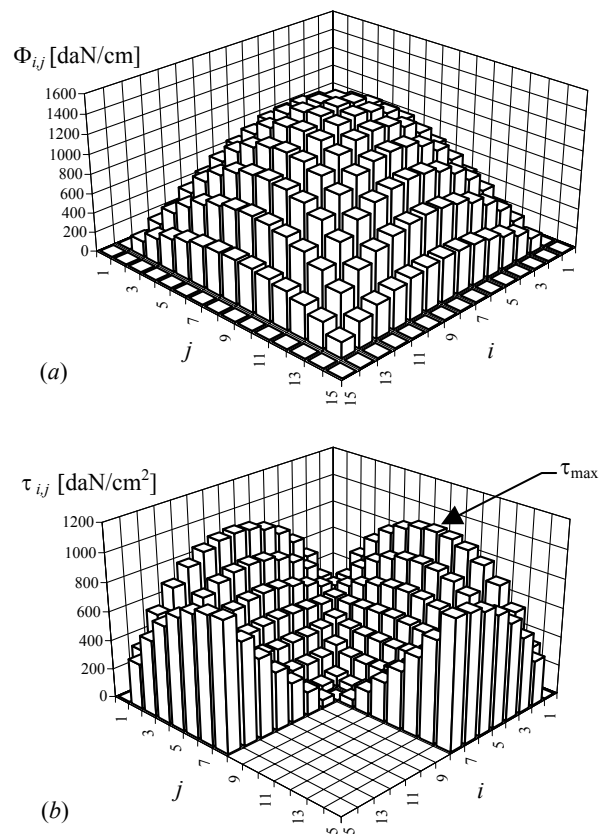


Figure 9. Example 1 – The results of the modeling: (a) the stress function; (b) the distribution of the shear stress (a quarter of 3D plot is removed for the sake of better visibility).

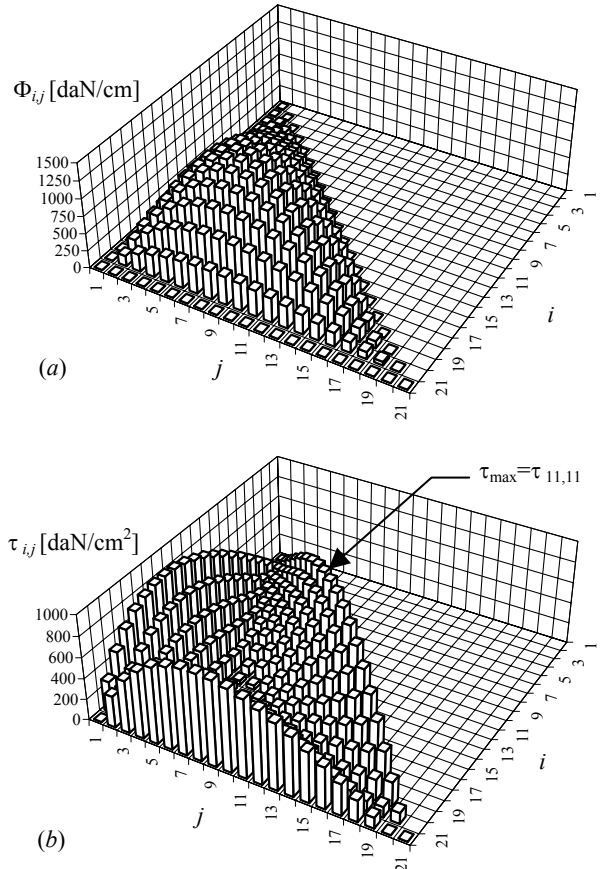


Figure 10. Example 2–The results of the modeling: (a) the stress function; (b) the distribution of the shear stress.

with a huge CNN model having the several thousands of cells (demanding a powerful computer for simulation), but only to demonstrate the application of the proposed method by means of reasonable model with only a few hundreds of cells (this can be simulated on a usual PC). Since solving this problem can be understood as "calibration" of the method, the interdependence between the accuracy of the obtained results and the size of model remains to be the subject of our further research.

Example 2. Solve the same problem as in example 1, assuming the square cross-section of bar is replaced by solid cross-section having the shape of right-angled triangle with sides $b=h=10$ [cm].

The cross-section of bar is modeled by a CNN with dimensions $M=21$ and $N=21$, having 441 cells, in total. However, the model itself consists of 231 active cells. The resulting distribution of stress function is depicted in Fig. 10a and the resulting distribution of the shear stress is depicted in Fig. 10b.

Both distributions are obtained in the same way as the respective distributions in the previous example. As is depicted in Fig. 10b, the maximum shear stress occurs in node (11,11) that is in the middle point of the hypotenuse, while other two peaks occur in the node (14,1), which lies on the first, and in node (21,8), which lies on the second side of the contour. The center of the twist is node (15,7) in which the shear stress is zero. This node belongs to the axis of symmetry of triangle, but obviously, it does not coincide with the centroid of triangle.

Example 3. Solve the same problem as in Example 1, if square cross-section of the bar is replaced by solid cross-section having the the shape depicted in Fig. 11.

This problem is modeled by a CNN with dimensions $M=18$ and $N=23$, having 414 cells in total, but model itself consists of 273 active cells. The resulting distribution of the stress function is depicted in Fig. 12a and the resulting distribution of the shear stress is depicted in Fig. 12b. Both distributions are obtained in the same way as distributions in the formerly presented examples.

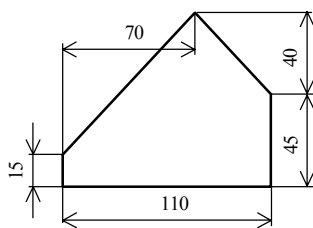


Figure 11. Example 3 – The cross-section of the bar (all measures are given in millimeters).

As is depicted in Fig. 12b, the maximum shear stress occurs in node (7,9), while other four peaks occur in nodes (18,14), (6,20), (12,23) and (16,1). All these nodes lie on the contour of the cross-section. The center of twist is in node (11,14).

6. CONCLUSIONS

Finding of the shear stress distribution in a twisted prismatic bar with solid cross-section in the shape of a complex irregular polygon presents a serious problem as is well known from the theory of elasticity. The key to

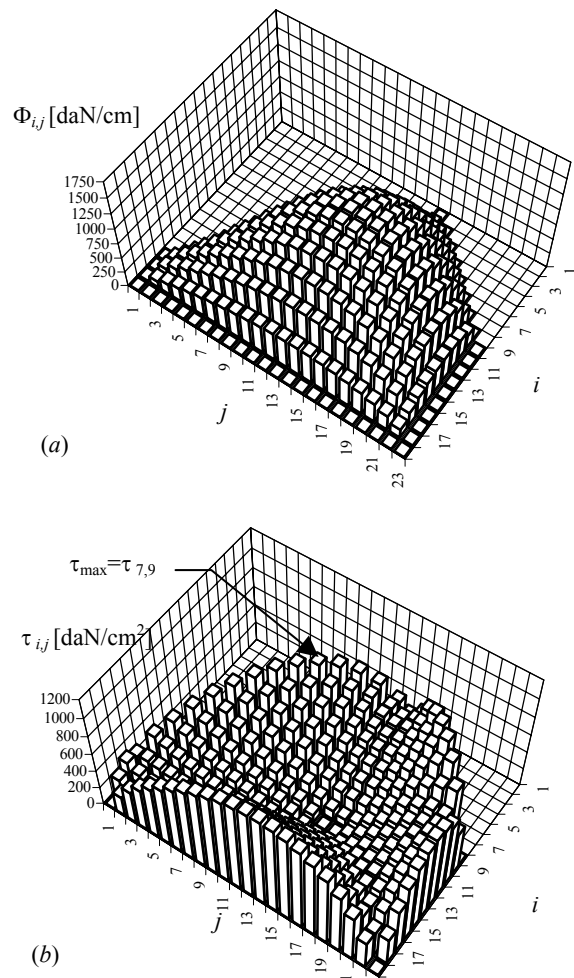


Figure 12. Example 3 – The results of the modeling: (a) the stress function; (b) the distribution of the shear stress.

the solution of this problem is to find the stress function. Consecutively, it will then serve for calculation of the shear stress distribution in the second step. The stress function appears to be the solution of Poisson's equation for given conditions of unambiguity, describing torsion of prismatic bars in terms of stresses. The same equation describes, also, the shape of the surface of a deflected flexible inextensible membrane exposed to uniform pressure. Modeling the problem by means of electrical networks is a possible way to find the stress function. The contemporary and effective method described in this paper enables determination of the stress function by means of original cellular neural network of Chua and Yang, which may serve to that purpose as very suitable analogous model. The predictive power of the method is presented by means of three illustrative examples. Their solutions presented here convincingly show that this approach can be applied straightforwardly and successfully in solving problems relating to twisted prismatic bars with complex cross-sections. The results obtained very well satisfy the expectations and usual provisions of contemporary practice. Moreover, the same method enables modeling and solving the Laplace equation for corresponding conditions of unambiguity, describing the torsion function of twisted prismatic bars (that is, the shape of warped cross-sectional surface of the bar).

Main benefits of the method are simple modeling and fast solving of problems, the possibility to achieve very high resolution of the model and thus very high accuracy of obtained results. In addition, CNNs are very suitable both for software implementation and simulation on PCs and for electronic implementation by conventional means (electric and electronic circuits, or VLSI technology [16], [17]). The application of the proposed method is expected in several branches of mechanical engineering.

REFERENCES:

- [1] Filonenko–Borodich M.: *Theory of elasticity*, Dover Publications, New York, 1965, p. 378.
- [2] Ružić D.: *The Strength of Structures*, Mechanical Eng. Faculty, Belgrade, 1995 (in Serbian).
- [3] Rašković D.: *The Strength of Materials*, Naučna knjiga, Belgrade, 1971, p. 426 (in Serbian).
- [4] Dally J., Riley W.: *Experimental Stress Analysis*, 2nd Edition, McGraw-Hill, 1978.
- [5] Uhlmann H.: *Grundlagen der Elektrischen Modellierung und Simulationstechnik*, Akademische Verlagsgesellschaft Geest & Portig G., Leipzig, 1977, p. 312.
- [6] Karplus W. J., *Analog Simulation – Solution of Field Problems*, (in Russian), *Издательство иностранной литературы* Moscow, 1962, p. 487.
- [7] Chua L. O., Yang L.: Cellular Neural Networks: Theory, IEEE Trans. on Circuits & Systems Vol. 35, No. 10, 1988, p. 1257–1272.
- [8] Chua L. O., Yang L.: Cellular Neural Networks: Applications, IEEE Trans. on Circ. & Systems, Vol. 35, No. 10, 1988, p. 1273–1290.
- [9] Henseler J., Braspenning J.: Membrain: A Cellular Neural Network Model Based on the Vibrating Membrane, Int. Jour. of Circ. Theory & Appl., Vol. 20, 1992, p. 483–496.
- [10] Szolgay P., Vörös G., Eross G.: On Applications of the Cellular Neural Network Paradigm in Mechanical Vibrating Systems, IEEE Trans. on Circ. & Systems – Part I: Fund. Theory & Appl., Vol. 40, No. 3, 1993, p. 222–226.
- [11] Szolgay P., Vörös G.: Transient Response Computation of a Mechanical Vibrating System Using Cellular Neural Networks, Proc. of the CNNA 94, Rome, 1994, p. 321–326.
- [12] Krstić I., Reljin B., Kostić P.: Solving direct linear problems of heat conduction by analogy with cellular neural networks, Proc. of the IV NEUREL 97, Faculty of E. Engg., Belgrade, 1997, p. 43–48.
- [13] Krstić I., Reljin B., Kostić P., Kandić D.: Solving the inverse linear problem of the heat transfer by cellular neural networks, Proc. of the X Int. Symp. on Theor. E. Eng., Magdeburg, 1999, p. 279–284.
- [14] Krstić I., Reljin B., Kostić P.: The cellular neural network to model and solve direct nonlinear problems of steady-state heat transfer, Proc. of the Int. Conf. on Trends in Comm.– EUROCON 2001, Vol. 2/2, Bratislava, Slovakia, 2001.
- [15] Puffer F., Tetzlaff R., Wolf D.: Modelling Almot Incompressible Fluid Flow with CNN, Proc. of IEEE Int. Workshop on Cellular Neural Networks and their Applications–CNNA '98, London, 1998, p. 78–82.
- [16] Reljin B., Kostić P., et al.: Single-amplifier CNN cell suitable for VLSI CMOS implementation, Int. Jour. Circ. Theory & Appl., Vol. 24, 1996, p. 649–655.
- [17] Yentis R., Zaghloul E.: VLSI Implementation of Locally Connected Neural Network for Solving Partial Differential Equations, IEEE Trans. on Circ. & Syst – Part I: Fund. Theory & Appl., Vol. 43, No. 8, 1996, p. 687–690.

ЦЕЛУЛАРНЕ НЕУРАЛНЕ МРЕЖЕ – АНАЛОГНИ МОДЕЛ ЗА АНАЛИЗУ НАПОНА ПРИЗМАТИЧНИХ ШТАПОВА ИЗЛОЖЕНИХ УВИЈАЊУ

И. Крстић, Д. Кандић, Б. Релџин

У најопштијем случају одређивање расподеле напона смицања у попречном пресеку призматичног штапа изложеног торзији представља озбиљан проблем који се може решити у два корака. Први се састоји у одређивању тзв. функције напона, а други у одређивању напона смицања преко поменуте функције. Функција напона јавља се као решење Поасонове парцијалне диференцијалне једначине за дате услове једнозначности, помоћу које се у теорији еластичности описује увијање призматичних штапова у функцији напона. Моделовање овог проблема помоћу електричних мрежа представља само један од неколико могућих начина за одређивање функције напона. У раду је дат један оригиналан метод примене целуларних неуралних мрежа за аналогно моделовање и одређивање функција напона увијених призматичних штапова са пуним полигоналним попречним пресецима. Тако добијене функције директно се могу даље користити за израчунавање резултујућих расподела напона смицања. Ефикасност формулисаног поступка илустрована је на три примера. Предложени метод се успешно може применити и на друге области машинске технике.